Investigations of Uraniumsilicide-based Dispersion Fuels for the Use of Low Enrichment Uranium (LEU) in Research and Test Reactors

S. Nazaré
Institut für Material- und Festkörperforschung

Kernforschungszentrum Karlsruhe

.

KERNFORSCHUNGSZENTRUM KARLSRUHE

Institut für Material- und Festkörperforschung

KfK 3372B

INVESTIGATIONS OF URANIUMSILICIDE-BASED DISPERSION FUELS FOR THE USE

OF LOW ENRICHMENT URANIUM (LEU) IN RESEARCH AND TEST REACTORS

S. Nazaré

Abstract

The work presents at the outset,a review of the preparation and proper-
ties of uranium silicides (U_3Si and U_3Si_2) in so far as these are rele-
vant for their use as dispersants in research reactor fuels. The expe-
rimental work deals with the preparation and powder metallurgical pro-
cessing of Al-clad miniature fuel element plates with U_3Si- and U_3Si-Al
up to U-densities of 6.0 g U/cm^3. The compatibility of these silicides
with the Al-matrix under equilibrium conditions (873 K) and the influence
of the reaction on the dimensional stability of the miniplates is described
and discussed.

Untersuchungen von Dispersionsbrennstoffen auf Uransilizidbasis für die Verwendung von niedrig angereichertem Uran in Forschungs- und Testreaktoren

Zusammenfassung

Es werden zunächst die in der Literatur bekannten Daten über die Her-
stellung und Eigenschaften von Uransiliziden (U_3Si und U_3Si_2) dargestellt.
Die experimentelle Arbeit befaßt sich mit der Herstellung und pulverme-
tallurgischen Weiterverarbeitung zu Al-umhüllten Miniatur-Brennelement-
platten mit U_3Si- und U_3Si_2-Al mit U-Dichten bis 6.0 g U/cm^3. Das Reak-
tionsverhalten dieser Silizide mit der Al-Matrix unter Gleichgewichtsbe-
dingungen (873 K) und der Einfluß der Reaktion auf die Dimensionsstabi-
lität der Platten wird beschrieben und diskutiert.

24. Juni 1982

Contents:

INVESTIGATIONS OF URANIUMSILICIDE-BASED DISPERSION FUELS FOR THE USE OF LOW ENRICHMENT URANIUM (LEU) IN RESEARCH AND TEST REACTORS

S. Nazaré

Kernforschungszentrum Karlsruhe
Institut für Material- und Festkörperforschung
Postfach 3640
D-7500 Karlsruhe

Introduction

Research and test reactors are being operated world wide with dispersion fuel element plates generally consisting of an UAl_x (mainly UAl_3) or U_3O_8-Al dispersion clad with an Al-alloy. Uptill recently, highly enriched uranium (HEU $\sim$ 93% 235-U) was used in such fuel element plates. With existing technology, fuel element plates are routinely fabricated using the well known picture frame technique up to U-densities of about 1.6-1.7 g U/cm^3 in the fuel dispersion. Concerns about the proliferation resistance of the fuel cycle have stimulated efforts to develop fuels that would permit the use of uranium with lower enrichment (LEU $\sim$ 20% 235-U). If major changes in the reactor performance are to be avoided, the 235-U-content in the fuel dispersion has at least to be retained at present levels. For the fuel development, this means that depending on the reactor, U-densities in the range of about 2.0-7.0 g U/cm^3 in the fuel dispersion have to be attained. Further use of the proven UAl_x or U_3O_8 phases is impeded by the fact that due their low U-densities (5.0; 7.1 g U/cm^3) the volume content of these phases in the dispersion would have to be raised to levels well beyond those that are fabricable ($\sim$ 45-50 vol.%). In practice,the limits lie at about 2.2 g U/cm^3 for UAl_x-Al and about 3.1 g U/cm^3 for U_3O_8-Al. Accordingly,the work was directed primarily towards the development of uranium silicide based fuels. From the fabrication viewpoint,the high U-density silicide based fuel would meet the LEU conversion requirements of practically all reactors.

The work was performed under the auspices of the German AF-Programm (Anreicherungsreduzierung in Forschungsreaktoren /1-3/). A similar program (RERTR Reduced Enrichment Research and Test Reactor Program) is also currently under way in the U. S. A. /4-8/.

Literature survey

A number of studies have been carried out in the past on uranium silicides, particularly U_3Si. They were however primarily directed towards the use of this silicide as a bulk fuel in natural uranium fueled power reactors. A review of very early work is presented in /9,10/. Initial investigations on U_3Si and U_3Si_2-Al /11,12/ dispersions were discontinued because of the good performance of the alternatives namely U_3O_8-Al and UAl_x-Al, and probably also because of fears that the presence of silicon might pose problems for the chemical reprocessing. Table I summarizes some of the properties that are pertinent to the use of silicides (U_3Si and U_3Si_2) as dispersants. The original work should be consulted for the proper assessment of the values given in the table, particularly for those properties that are extremely sensitive to minor changes in the chemical composition and/or microstructure.

U_3Si

The U-Si phase diagram (fig.1) reveals the occurrence of a large number of intermetallic phases /13-15, 21-25/. The U_3Si-phase is formed by the following peritectoid transformation at 1198 K:

$$3 U + U_3Si_2 \rightarrow 2 U_3Si$$
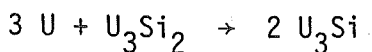
It exists either in the cubic structure /15/ above about 1033 K or as a face centered tetragonal below this temperature /14/. The transition results in a twinned martensitic structure consisting of bands and subbands as a result of double shear /26/. However, it is possible to produce a non-martensitic structure when the peritectoid reaction occurs below about 923 K /27-29/. Since the reaction rate drops significantly with tempera-

ture,longer annealing times are obviously required at lower temperatures.

Due to the interest in this compound for natural uranium fueled power re-
actors, considerable efforts have been made to develop adequate prepa-
ration techniques. Induction melting in graphite crucibles /30/ (some-
times with a lining of beryllia or zirconia) has been generally adopted
as against arc melting which does not easily yield a homogeneous product
and has size limitations /10/. Hyperstoichiometric compositions are ge-
nerally chosen to compensate for silicon losses during melting. Since
the peritectoid transformation is extremely sluggish, the microstructure
of the solidified melt consists predominantly of αU and U_3Si_2 as well as
a small rim of U_3Si. Subsequent heat treatment for prolonged periods is
necessary to complete the reaction.

As is also common in most eutectoid reactions, the most rapid transformation
rate occurs at some degree of undercooling below the equilibrium tempe-
rature. The TTT diagram reveals two maxima at 1093 K and 1043 K /31/. A
suitable annealing temperature seems to be about 1073 K. It can be expected
that the primary U_3Si_2 grain size plays an important role in the kinetics
of the solid state reaction. An empirical equation for the width of the
U_3Si rim formed /32/ is given as:

$$X = 5.65 \ t^{0.39} \quad (T = 1073 \text{ K, grain size} \leq 30 \text{ microns})$$

with X = rim thickness in microns
      t = heat treatment time (hours)

The rate of growth is controlled by the interdiffusion of silicon and
uranium. The activation energy in the temperature range of 893-1033 K is
209 ± 4 KJ/mole /33/.

Carbon is considered to be an important impurity. Concentrations of 2000 ppm
lower the peritectoid temperature /13,34/ and form regions of three-phase
equilibrium between U or UC, U_3Si_2 and U_3Si /35/, which exists between 1063 and
1133 K. Increasing carbon contents lower the optimum transformation tem-
perature (at 80 ppm 1098 K; at 2000 ppm 1043 K). Experimental evidence
seems to suggest, however, that lowering transformation temperatures does

not significantly affect the transformation rate, possibly because the presence of carbon increases the diffusivity /34/.

The mechanical properties of U_3Si are difficult to compare because the quality of the material has varied considerably. At room temperature U_3Si shows ductility under compression or rolling. Yielding takes place below 600 N/mm^2; fracture occurs at a stress level of about 1700 N/mm^2 with 17% deformation /13,34,37/. In tension, U_3Si exhibits a brittle behaviour at room temperature. The fracture stress is about 240 N/mm^2, increasing to 390 N/mm^2 at 523 K /38/. In the temperature range of 348-593 K a sharp pseudo yield point is observed at a stress level of about 240 N/mm^2 independent of temperature. The stress strain curve reveals two stages. The initial deformation ends with a sharp elastic-plastic transition and is followed by strain hardening leading to fracture /38/. The plastic deformation is accompanied by detwinning of the martensitic structure.

Investigations of recovery and recrystallization /39/ reveal that the recovery of U_3Si (3.98 wt.-% Si, 600 ppm carbon) with 10% coldwork begins in the range of 673-723 K and is complete after 6 hours at 923-973 K. A small change in the silicon concentration (3.98 wt.-% to 3.27 wt.-%) has no effect on the process, but a decrease in the carbon content (from 600 ppm to 140 ppm) decreases the recovery temperature. This may be the result of the pinning effect of the finely dispersed carbide on the dislocation network.

The irradiation stability of bulk U_3Si and U-Si-Al alloy (3.5 wt.-% Si, 1.5 wt.-% Al; U_3Si(Al) with U_3Si_2 and UAl_2) fuel clad with zirconium alloys and containing a central axial void to accomodate swelling has been reported in the past /40-43/. The effect of temperature on swelling has been established /44,45/,and the mechanism is considered to be controlled by the nucleation and growth of voids. Experimental evidence seems to point out some additional source of instability due to irradiation:

-   the micro-twinned structure of U_3Si in destroyed by irradiation below 373 K at exposures above $6 \cdot 10^{16}$ f/cm^3 /46,47/

- the ordered tetragonal phase transforms to a disordered face centered cubic structure upon irradiation at 473-573 K at exposures above 10^{17} f/cm^3 /47-49/.

It might be pointed out, in the context of the irradiation behaviour, that the irradiation stability of the bulk dispersant, important though it is, is not in itself sufficient to guarantee the stability of the combination. The irradiation stability of dispersions is probably a complex function of various properties of the dispersant and the matrix together. For example a proven fuel like UO_2 has not proved to be very stable when used as a dispersant in UO_2-Al dispersions.

U_3Si_2

In comparison to U_3Si, there is much less information available on the U_3Si_2 phase. This congruently melting compound does not seem to have a homogeneity range. It has been prepared by repeated arc melting in inert gas /18/ or vacuum induction melting in ceramic lined graphite crucibles /50/. Reaction hot-pressing of stoichiometric mixtures of elementary powders resulted in porous pellets which densify at about 1723 K /51/.

Sintering of U_3Si_2 pellets (compaction pressure 15 KN/cm^2) at 1632 K in vacuum or inert gas for 6 hours yields densities of about 96% TD. Hot pressing in alumina lined graphite dies at a pressure of 9 KN/cm^2 results in products with 98% TD /52/.

In addition to the property data presented in Table I, further available information on the mechanical properties of U_3Si_2 is not on fully characterised material to be very meaningful. The scatter is probably due to the brittle nature of this compound and varying porosity. The stress at fracture varies between 140-280 N/mm^2; the static modulus of elasticity between 51.0 KN/mm^2 and 142.0 KN/mm^2 /18,53/.

A single capsule irradiation test on silicon-deficient bulk U_3Si_2 (7.07-7.17 wt.-% Si) at high centerline temperatures (1243 K) showed volume increases of about 12% after a burnup of $4.2 \cdot 10^{20}$ f/cm^3 /18/. Previous irradiation data on miniature U_3Si_2-Al dispersion fuel plates (1.3 g U/cm^3, HEU), which as a result of low volumetric content of the dispersed phase

(12 vol.-% U_3Si_2) had practically no voids to accomodate swelling, reveal a volume increase of 6.6% after a burnup of $13.4 \cdot 10^{20}$ f/cm^3 at an average temperature of 397 K /12/.

Interactions in the ternary U-Si-Al system

For the use of the silicides as dispersants in an Al-matrix, the compatibility between the dispersed phase and matrix can be of major importance.
The results available are the products of the work carried out in the past with a view to stabilizing the UAl_3 phase in the U-Al system, by ternary additions /54-57/. It was found that silicon additions of >3 wt.-% in U-Al alloys (48 wt.-% U) effectively suppress the peritectic reaction which leads to the formation of UAl_{4+x}. The explanation offered was that in the ternary system these alloys lie in a two phase region of thermodynamic equilibrium between $U(Si,Al)_3$ and Al. It was assumed that the cubic phases UAl_3 and USi_3 form a continuous series of solid solutions; silicon occupying the Al-sites in the UAl_3 lattice.

Phase equilibria studies have been carried out in the $U-UAl_2-U_3Si_2$ portion of the U-Si-Al system /58,59/.
Isothermal sections at 1223, 1123 and 923 K reveal no major solubilities for aluminium in U_3Si and U_3Si_2 and for silicon in UAl_2. The quasibinary $U_3Si_2-UAl_2$ system is a simple eutectic. Microprobe analysis was used to investigate the solid state reaction between U_3Si and Al.
The reaction in essentially complete with in 24 hours at 873 K. The main reaction product was identified as $U(Si,Al)_3$. Traces of an unidentified phase were reported on the basis of X-ray diffraction data /60/.

Experimental work

Preparation of the silicides

Induction melting in alumina crucibles as well as arc melting in water cooled copper crucibles were used to prepare the U_3Si and U_3Si_2 compounds. In both cases, slightly hyperstoichiometric compositions were chosen; being 4.0 wt.-% Si in the case of U_3Si and 7.4 wt.-% in the case of U_3Si_2. Typical microstructures of U_3Si are shown in fig.2. They reveal, as expected, primary U_3Si_2 and an eutectic of U_3Si_2 and α-uranium.

A comparison of fig.2a and 2c shows that the rapid quench obtained during arc melting leads to a finer primary grain size of U_3Si_2 than the one obtained by induction melting and furnace cooling. Furthermore, in the case of the samples prepared by induction melting, the formation of a small amount of uranium aluminides due to the aluminium pick up from the alumina crucible can be seen. The structures of the U_3Si_2 phase (fig.3) reveal a predominantly single phase product, with very small amounts of USi. No significant differences are observed between the arc and induction molten material.

The as-molten U_3Si was subjected to a homogenisation heat treatment mainly at 1073 K for 72 hours, in a vacuum of $\leq 10^{-5}$ mbar for arc cast material, 350 hours for induction molten material. It is known, that depending on the primary U_3Si_2 grain size and carbon content, this heat treatment is sufficient to carry the peritectoid formation of U_3Si essentially to completion. The microstructures of the hyperstoichiometric product after heat treatment (figs.2b,d and e), reveal a two phase structure, consisting of U_3Si_2 in a matrix of U_3Si. Practically no free α-uranium is detectable in the microstructure.

Although there is not, in principle, an obvious need, the U_3Si_2 melts were also subjected to a homogenising heat treatment similar to U_3Si (mainly 1073 K, 72 hours, $\leq 10^{-5}$ mbar). As can be seen from the microstructures in fig.3, there is no marked change after heat treatment except for grain coarsening. The cracks that are visible, are an indication of the brittleness of this compounds as compared to U_3Si.

Powder metallurgical processing of the silicides

For the preparation of the miniature fuel element plates it is necessary to comminute the molten material to a desired particle size.
In the commercial fabrication of UAl_x and U_3O_8-Al dispersion fuel plates, it is common practice to use particle sizes for the dispersed phase in the range of 44-150 μm (75 wt.-%) allowing only a limited quantity (25 wt.-%) of finer powder (<44 μm). This requirement arose from the concept that under irradiation, the zones of fission fragment recoil should not overlap /61,62/, so that a continuous undamaged metallic matrix is preserved

for the dissipation and transport of fission heat. In addition, the ductility and thickness of the ductile matrix rim around the fissionable particles is thought to contribute towards the prevention of crack initiation and propagation from stresses that develop due to particle swelling. Although there is evidence /63/ that at low volume contents of the dispersed phase (HEU, e.g. 38.8 vol.-% UAl_x) the stability and swelling are not influenced by the particle size (size fraction <44 μm) but primarily by the porosity in the particles and in the dispersion, the specifications have been retained because of the proven stability of fuels with these characteristics. It should be mentioned, that in thermodynamically unstable dispersions, the reaction kinetics could be accelerated by using a large amount of fine powder. In addition, the thermal conductivity of the dispersion might be decreased when the particle size is reduced, specially at high contents of the dispersed phase.

For the experiments outlined here a narrow particle size range of 63-90 μm was selected. Although this particle size range may neither be important, desirable nor economical in commercially fabricated fuel elements, it was retained with a view to keeping possible surface and interfacial phenomena unchanged.

A jaw crusher was used in the first step of the communition which was carried out in an argon filled glove box, followed by grinding in a WC-Co lined "shatterbox", with intermittend sieving. Whereas U_3Si_2 comminutes easily tending to be extremely friable, difficulties are encountered in the grinding of U_3Si because of the toughness of the material. There is therefore a need to develop improved comminution methods for the generation of large batches of powder. The chemical composition and powder characteristics of the milled silicide powders are given in Table II along with those of the Al-matric powder.

Further processing of the powders to produce Al-clad miniature fuel plates (plate dimensions 220·40·1.3 mm^3; nominal meat dimensions 200·30·0.5 mm^3) was carried out in the following well known steps:

- Blending with Al-powder at 80 rpm for 2 hours. Care has to be taken at this stage to avoid segregation of the powders.

- Compaction of the powder blend to pellets at a pressure of 50 KN/cm^2. Only the surface of the die were lubricated with a solution of stearic acid in petrolether.

- Fitting of the compact in the cleaned picture frame followed by welding of the cover plates.

- Hot rolling at 773 K in a series of well defined passes with intermediate heating.

- Cold rolling to final dimensions, blister testing (773 K, 1 hour) shearing to size, and finishing operations.

The procedure described was used to prepare Al-clad U_3Si-Al fuel plates with U-densities of 3.0, 4.0 and 6.0 g U/cm^3 in the dispersion. Similarly fuel plates with U_3Si_2-Al and U-densities of 3.0, 4.0 and 4.5 g U/cm^3 in the dispersion were prepared. Thus the basis was established for the commercial fabrication of full size prototype fuel element plates with U_3Si_2-Al and an U-density of 4.75 g U/cm^3 (clad with AlMg$_1$). These plates will be operated in the ORR-Reactor.

Fig.4 shows the microstructures of the miniature fuel as well as full size fuel plates. The fuel homogeneity was within the usual limits and the requirements of minimum cladding thickness (0.2 mm) could be met. A comparison of the microstructure of the U_3Si- and U_3Si_2-Al plates reveal that due to the brittle nature of the U_3Si_2-phase, particle break up occurs during rolling.

The core thickening that usually occurs at the ends of the fuel plate (dog boning) is of concern since it reduces the cladding thickness in this area, whilst increasing fuel concentration which may lead to excessive temperatures. The use of tapered compact ends along with alloyed Al-cladding should alleviate this problem. Probably the U-density in these dispersions could be increased to slightly higher levels.

Compatibility of the uranium silicides with the Al-matrix

The objectives of the investigations outlined here were primarily:

1.   To extend the present knowledge of the ternary U-Si-Al system
      to those regions that are of relevance for the fabrication and
      in-pile behaviour of the dispersions.

2.   To investigate the reaction behaviour of roll bonded disper-
      sions particularly with regard to the dimensional changes that
      occur in the fuel plate as a consequence of the reaction.

Equilibrium investigations

The samples for the investigations of the reaction behaviour under equi-
librium conditions were prepared by arc melting of the elements in an
argon atmosphere ($\sim$ 5 bar). The initial compositions, which have since
been extended, were chosen to correspond to 20, 30, 40 and 50 vol.-%
U_3Si or U_3Si_2-Al. Fig.5 shows the microstructure of the U_3Si-Al samples
in the as-cast state as well as after a heat treatment at 873 K ($\sim$ 33 days).
It is possible that on account of the low diffusivity at these tempera-
tures, the annealing times were not sufficient to attain complete equi-
librium. This would be particularly true for the formation of UAl_{4+x},
whose formation below 1018 K is known to be extremely slow /64/. How-
ever,these conditions were judged to be of practical importance for our
case, and it is unlikely that the main results would vary substantially
if the heat treatment was carried out for longer times. Samples corres-
ponding to 20 and 30 vol.-% U_3Si (figs.5a and 5c) reveal in the as cast
condition two phases namely $U(Si,Al)_3$ and Al. After heat treatment an
additional phase namely UAl_4 with silicon in solution appears as a rim
around the original $U(Si,Al)_3$ grains (figs.5b and 5d). The sample corres-
ponding to 40 vol.-% shows two predominant phases namely $U(Si,Al)_3$ and
UAl_2 (figs.5e and 5f). There is evidence that indicates that the dark
precipitates clearly seen in figs.5e and 5f (some signs are already
evident in figs.5c and 5d) are caused by the temperature dependent so-
lubility of silicon in UAl_2 /59/ and UAl_3. Available results show a
miscibility gap at low temperatures in the quasi binary UAl_3-USi_3 system
(figs.6a and 6b). Heat treatment at 873 K does not change substantially

the amount or morphology of these phase. In the sample corresponding to 50 vol.-% U_3Si, three phases can be seen the microstructure $U(Si,Al)_3$, $UAl_2(Si)$ and $U_3Si_2(Al)$ in both the as cast and annealed state.

The situation is somewhat different in the case of the U_3Si_2-Al samples (fig.7). Samples corresponding to 20, 30 and 40 vol.-% U_3Si_2 reveal in the as cast as well as heat treated state mainly two phases namely $U(Si,Al)_3$ and Al (with small amounts of silicon in solution). Here again there is some evidence of miscibility gap in the UAl_3-USi_3 quasi binary system leading to precipation at the grain boundaries (figs. 7e and 7f). The silicon content in these cases is sufficient to stabilize the $U(Si,Al)_3$ phase and prevent UAl_{4+x} formation. This is a well known fact from early work on the stabilisation of UAl_3 phase in cast U-Al alloys /54-57/. The samples corresponding to 50 vol.-% U_3Si_2 reveals a three phase structure in the as cast and heat treated state namely $U(Si,Al)_3$, $U_3Si_2(Al)$ and probably $USi_3(Al)$.

The results described above are summarized in Table III. It includes X-ray diffraction date of the heat treated samples obtained with standard Guinier procedures. Selected sample have also been analysed with a microprobe. The compositions determined are also given in Table III. Microhardness measurements using an indentor load 0.15 N were carried out and are given in the table.

Based on this limited data and literature available, it is possible to propose tentatively an isothermal section at 873 K in the U-Si-Al system (fig.8). Further experiments are underway to define the precise limits of the phase regions and clarify the situation in the U-rich portion of the system,

It must be mentioned in this context, that probably equilibrium conditions will not be generally attained during the normal operation conditions and life of the fuel. However, it is well known, that the diffusion reactions are enhanced in a neutron environment in UO_2-Al, UAl_x-Al and U_3O_8-Al fuels /64-70/. Smaller particle sizes of the dispersed phase and surface energy effects could also significantly increase the reaction rate assisting the attainment of equilibrium. The phases formed under equilibrium conditions could be important during a LOCA.

Influence of the reaction of the dimensional stability of roll bonded miniature plates

In order to investigate the reaction behaviour of the silicide disper-
sions, small miniature plates with a pure Al-cladding were fabricated
using the procedures outlined before. Cylindrical pellets (10 mm $\emptyset$,
2,5 mm high) with 26.7 vol.-% U_3Si and 35.4 vol.-% U_3Si_2 were used.
This corresponds to an U-density of 4.0 g U/cm^3 in the meat. The si-
licide and Al-powders were degassed at 873 K in a vacuum <10^{-5} mbar for
4 hours. The particle size of the silicides was within the sieve range
of 63-90 microns. The miniplate dimensions were, 70·15·1.3 mm^3, the
nominal meat-thickness was 0.5 mm; the nominal cladding thickness being
0.4 mm. The density of the pellets prior to rolling was about 93% T.D.
for the U_3Si-Al-, being 95% T.D. for the U_3Si_2-Al-dispersion. Immersion
density measurements of the roll bonded plates revealed that roll bonding
increased the density in the fuel meat to about 99% for the U_3Si-Al-
dispersion.

The samples were then heat treated in evacuated pyrex tubes for times
up to about 2000 hours. A control specimen containing only a meat of
pure Al was also heat treated along with the specimen in each case. This
was done with a view to determining whether adsorbed or trapped gases in
the Al-matrix alone could be the cause of swelling. Dimensional and vo-
lume measurements by immersion were carried out before and after the
heat treatment. Fig.9 shows the change in thickness of the plates after
heat treatment at 523 K, 623 K and 723 K plotted as a percentage of the
total plate thickness, generally 1.3 mm. The volume changes in the fuel
meat and plate follow a similar pattern. It can be observed from fig.9
that the fuel plates show practically no dimensional changes at 523 K
for annealing times up to 1800 hours. This could mean that up to this
temperature very little or practically no reaction takes place. At 623 K
fuel plates with U_3Si as the dispersed phase show dimensional changes up
to about 2%; however, the dimensional changes measured are lower with
U_3Si_2 than with U_3Si. The situation changes significantly at 723 K. Not
only are substantial dimensional changes measured, but there also appears
to be an inversion in the magnitude and rate of dimensional change. At
this temperature larger dimensional increases occur with U_3Si_2-Al than
with U_3Si-Al.

Selected photographs of the samples after heat treatment are shown in fig.10. Apart from providing a qualitative picture of the volume increase, they also show that the volume increase occurs only in the meat region of the fuel plate. Obviously, since the control plates with pure aluminium did not show any swelling at all temperatures the volume increase is caused by the phenomena associated with the reaction between the dispersed phase and the matrix.

Standard X-ray diffraction procedures (Guinier), metallography and energy dispersive X-ray analysis were used to identify the reaction products. After the 2000 hours anneal, the major reaction product identified in U_3Si-Al was $U(Si,Al)_3$ with a lattice parameter of 425.6 pm, the microhardness being 311±19 VPN at 0.05 N load. In the case of U_3Si_2-Al, the lattice parameter of the reaction product $U(Si,Al)_3$ was 423.2 pm, the microhardness being 260±57 VPN at 0.05 N load. It seems, that from the reaction kinetics viewpoint, the $U(Si,Al)_3$ phase shows preferred growth over the other possible phases. Free aluminium was identified in both cases. Some weak diffraction patterns could be possibly traces of $UAl_4(Si)$ in the case of U_3Si-Al. There were also traces unreacted U_3Si or U_3Si_2.

Metallographic analysis was carried out in all annealed specimens. Vacuum infiltration was used to prevent breakout of the material during the standard grinding and polishing operations. Fig.11 is a set of micrographs (U_3Si-Al) that shows the microstructure after heat treatment at 723 K for times up to 2000 hours. The main reaction product $U(Si,Al)_3$ appears greyish, the unreacted material is dark. Aluminium is seen as a white phase. It is interesting to note the large voids that are formed around the reacting particles. These could be an indication of a Kirkendall type of porosity which arises due to large differences in the partial diffusion coefficients of the reacting species. This type of porosity could contribute to the large swelling that occurs in the specimens which is much greather than the one predicted by merely considering the differences in the specific volumes of the theoretically dense reaction products and reactants. Similar volume increases have also been observed in the past with UO_2-Al dispersions /73/.

It is more likely that adsorbed gases that are released as a result of the reaction contribute to the swelling when the pressure build

up at higher temperatures causes creep in the Al-matrix /73/ and cladding. In such a case, the values for the dimensional changes will be dependent on the matrix and cladding high temperature strength. Accordingly the values reported here are likely to be reduced if alloyed cladding material is used. Experiments are under way to further clarify the mechanisms that contribute to the abnormal swelling observed.

Fig.12 shows a series of micrographs for the U_3Si_2-Al reaction. In this case also the reaction product is grey, the remaining U_3Si_2 is dark; Al being the white phase. The comments made for the U_3Si-Al are also valid here except for one difference that has been observed between the two cases. A comparison of the micrographs of the two sets (figs.10 and 11) reveals, a difference in the type of attack between the two cases. Whereas in the case of U_3Si_2-Al an even reaction zone is formed around the reacting particles, the U_3Si particles are breaking up into smaller grains. Although the interpretation of the reaction mechanism is powder reactions may be obfuscated by morphological and surface energy effects, this could mean that in the U_3Si_2-Al case volume diffusion is the rate determining step, whereas in the case of U_3Si-Al the grain and subgrain boundaries within the particles (fig.10a) which are probably formed as a result of the martensitic transformation provide initially preferred diffusion paths for Al-transport. This effect may also be only typical for the particle size ranges used in these experiments.

It is somewhat surprising that the high temperature U_3Si_2 phase - judged on the basis of dimensional changes alone - appears to be more reactive at higher temperatures than the low temperature U_3Si-phase. Hot stage microscopy experiments performed with pressed pellets, reveal the opposite. It is very likely that two factors contribute to the inversion in the swelling behaviour observed:

- Firstly due to brittle nature of the U_3Si_2 phase, particle break up occurs during rolling, shifting the particle size to lower ranges than the one used initially (63-90 μm). Particle size measurements carried out in samples after rolling show a mean U_3Si_2 particle size of only about 40 μm. This particle break up does not occur in the case of the ductile U_3Si-phase. Thus the interfacial contact area is increased beyond the normal amount that is the result of the higher volume con-

centration (35.4 vol.-% U_3Si_2-Al; 26.7 U_3Si-Al for 4.0 g U/cm^3).

- Secondly if the gas pressure build up is the main cause of swelling, the lower matrix content in the U_3Si_2-Al dispersions would mean lower strength, higher creep, and thus larger swelling at higher temperatures.

Measurements carried out in a push rod dilatometer provide additional evidence for the aforementioned effect. The samples in this case, were sections of miniature plates, which were without clad constraint in two directions. The measurements were carried out in high purity argon, the change in thickness of the plate was measured perpendicular to the rolling direction. Fig.13 shows the measured changes in length after attaining isothermal conditions.

At high temperatures, the onset of isothermal swelling is somewhat arbitrary since swelling already sets in during heating before isothermal conditions are reached. Some bowing of the sample was observed and the recorded length change includes undefined amounts of this factor.

After a temperature dependent incubation period, changes in length are observed in both cases. The absolute values which apparently increase with temperature are another indication of the aforementioned effect caused by gas pressure swelling.

An assessment of the thermal conductivity of the dispersions

Theoretical considerations, which may be considered to be state of the art now, permit an estimate of the conductivity of the dispersions if the conductivities of the phases are known (for details see /74-76/). It could be altered during operation due to the formation of reaction products and changes in the conductivity of the phases during exposure.

Discarding the simplest case of a series or parallel array of the phases which provide the outer-most upper and lower bounds (first order bounds) for the conductivity of the dispersion, we can consider the next simpler

case of an two-phase isotropic material implying statistical orientation of the phases. For this case we have:

$$\phi_C = \phi_1 \frac{3\phi_2 + 2(1 - c_2)(\phi_1 - \phi_2)}{3\phi_1 - (1 - c_2)(\phi_1 - \phi_2)} \qquad (1)$$

$$\phi_C = \phi_2 \frac{3\phi_1 + 2c_2(\phi_2 - \phi_1)}{3\phi_2 - c_2(\phi_2 - \phi_1)} \qquad (2)$$

with ϕ = thermal conductivity

   C = concentration (volume fraction)

Indices: denote: c = dispersion,

             1, 2 = phase 1 or phase 2.

For our particular case, since the thermal conductivity of aluminium is always greater than the one of the silicides, equation (1) gives the upper bound and equation (2) the lower bound. These bounds are shown in fig.14, and have been calculated with values of 1.9, 0.175 and 0.084 $W\,cm^{-1}K^{-1}$ for the Al, U_3Si and U_3Si_2 phases respectively. It can be seen from the figure that these bounds (second order) are relatively narrow when the conductivities of the phases do not differ substantially as is the case with U_3Si and Al.

It is reasonable to assume in our case, that it is probable that the dispersion will have an Al-matrix, keeping in mind that otherwise, the fabrication would be difficult.

With this additional assumption (Al-Matrix) and isotropic material we have (third order bounds):

$$1 - C_D = \frac{\phi_C - \phi_D}{\phi_M - \phi_D} \left[\frac{\phi_M}{\phi_C}\right]^{1/3} \quad \text{for } \phi_M > \phi_D \qquad (3)$$

with indices C, M, D $\hat{=}$ dispersion, matrix and dispersed phase respectively.

The above equation, which is likely to provide a good estimate thermal conductivity of the dispersion provides values too close to those of equation (1) to be shown in fig.14.

It can be seen from fig.14, that inspite of the slightly lower thermal conductivity reported for U_3Si_2 compared to U_3Si (see table I), as long the Al-matrix is retained only minor differences in the thermal conductivities of the U_3Si and U_3Si_2-Al dispersions are predicted by the equations.

Since the fuel dispersion generally contains substantial amounts of porosity, the values obtained with the aid of the above equations have to be corrected for porosity.

For an isotropic porous material we have (third order bounds)

$$\phi_P = \phi_M (1 - P)^{1.5} \quad \text{(upper bound)} \tag{4}$$

$$\phi_P = \phi_M (1 - P)^3 \quad \text{(lower bound)} \tag{5}$$

with   P = fractional porosity
indices denote: M = matrix;   P = porous material.

Thus, a series of values can be generated for the thermal conductivity of the porous dispersion for the three cases where the porosity is only located in the dispersed phase or matrix or partly in both.

Conclusions

1. Arc or induction melting with subsequent homogenisation in inert gas can be used to prepare U_3Si and U_3Si_2. Whereas the cominution of U_3Si to generate powder of the size range desirable in dispersion fuel elements still poses problems because of the toughness of this material; U_3Si_2, which is extremely brittle, is easily comminuted. State of the art picture frame technology can be adopted to fabricate Al-clad miniature fuel element plates to U-density levels of 6.0 g U/cm^3 for U_3Si-Al and 4.75 g U/cm^3 for U_3Si_2-Al. It should be possible to raise these limits slightly, whilst maintaining currently used specifications.

2. U_3Si- and U_3Si_2-Al are thermodynamically unstable. The type and amount of reaction products (uranium aluminides) formed, obviously varies with concentration and temperature and can be predicted from the ternary phase diagramm. The uranium aluminides UAl_2, UAl_3 and UAl_{4+x} dissolve substantial amounts of silicon at higher temperatures, the solubility is however, in the case of UAl_2 and UAl_3 temperature dependent.

3. In the case of roll bonded miniature fuel element plates, the reaction is accompanied by dimensional changes that are restricted to the core region of the plate. Whereas U_3Si- and U_3Si_2-Al dispersions are practically dimensionally stable at 523 K ($\sim$ 2000 hours) indicating none or very little reaction at this temperature, substantial dimensional changes occur after heat treatment at higher temperatures. It is probable that liberation of a gaseous species is a prime contributor to this swelling. There are indications, that under thermal conditions alone, the large number of grain boundaries present in U_3Si provide preferred diffusion paths for the Al.

4. The relatively high thermal conductivity of the silicide particularly in comparison to the oxide U_3O_8, as well as the proven irradiation stability of the uranium aluminides - which could be formed as reaction products during operation - are likely to contribute significantly towards the irradiation stability of the fuel plate under normal operation conditions. It should be borne in mind, that whilst using

LEU fuel, the fission events in the individual dispersed particle
are reduced by a factor of about $\sim$ 5. Analysis of the postirradi-
ation data of the irradiation tests planned and under way in the
AF- and RERTR-Programms should provide answers to the question
whether the fissions in the particle or the fission rate in unit
volume is the main factor which determines the metallurgical pro-
cesses in the dispersion.

5. If the problem of cominution of U_3Si can be solved on a commercially
viable basis, if the irradiation stability to the desired burn up
is proven and if the reprocessing of the spent fuel posess no techni-
cal problems, a basis would be established for the LEU-conversion of
practically all operating research and test reactors.

References:

/1/   IAEA - TECDOC 23 (1980)

/2/   Thamm G., Proceedings Reaktortagung 1980, 965

/3/   Nazaré S., Koch K.H., Proceedings Reaktortagung 1982, in print

/4/   Travelli A., Seminar on Research Reactor operation and Use,
        Jülich, Germany 1981, IAEA-SR-77/22

/5/   Stahl D., ibid, IAEA-ST-77/23

/6/   Snelgrove J.L., ibid, IAEA-SR-77/24

/7/   Domagala R.F. et al., International Meeting on Development
        Fabrication and Application of Reduced-Enrichment-Fuels for Re-
        search and Test Reactor ANL, Nov. 1980

/8/   Copeland G.L., Martin M.M., Nuclear Technology 56 (1982) 547

/9/   Steinkopff H., Thümmler F., Kernenergie 2 (1959) 1105

/10/   Bardsley J., AAEC/TM 487 (1968)

/11/   Graber M.J. et al., IDO - 17037 (1964)

/12/   Francis W.C., Moen R.A., IDO - 17218 (1966)

/13/   Kaufmann A. et al., Trans. AIME 209 (1957) 23

/14/   Blum P.L. etal., C.R. Acad. Sci. 260 (1965) 5538

/15/   Zachariasen W.H., Acta Cryst. 2 (1949) 94

/16/   Barin I.,Knacke O.,Kubashewski O., Thermochem. Prop. of inorganic Sub-
        stances, Supplement (1977), Springer

/17/   Bitsianis G., CT-3309 (1945)

/18/   Schmizu H., NAA-SR-10621 (1965)

/19/   Loch L.D. et al., BMI-1125 (1956)

/20/   Isserow S., NMI-1145 (1956)

/21/ De Voogth D. et al., J. Nucl. Mat. 46 (1973) 303

/22/ Boucher R.R., J. Appl. Cryst. 4 (1971) 326

/23/ Kimmel G., Nadiv S., Acta Cryst. 331 (1975) 1351

/24/ Brown A.A., Norreys J.J., Nature 183 (1959) 673

/25/ Brown A.A., Norreys J.J., Nature 191 (1961) 61

/26/ Ambler J. R.F., J. Nucl. Mat. 22 (1967) 112

/27/ Lombard L. et al., J. Nucl. Mat. 37 (1970) 121

/28/ Bethune B., Bevis M., J. Nucl. Mat. 44 (1972) 347

/29/ Kimmel G. et al., J. Nucl. Mat. 89 (1980) 402

/30/ Chalder G.H., AECL-2874 (1967)

/31/ Honma T. et al., Bull. of the Research Inst. of Mineral Dressing
and Metallurgy, Tokoku Univ. Sendai 35 (1979) 136

/32/ Berthiaume L.C., Wyatt B.S., AECL-3222 (1968)

/33/ Kimmel G. et al., J. Nucl. Mat. 40 (1971) 242

/34/ Wyatt B.S., J. Nucl. Mat. 27 (1968) 201

/35/ Guinet P. et al., J. Nucl. Mat. 21 (1967) 21

/36/ Isserov S., Trans. AIME 209 (1957) 1236

/37/ Kimmel G., Nadiv.S., J. Nucl. Mat. 54 (1974) 299

/38/ Kimmel G. Nehema E., Scripta Metallurgica 13 (1979) 361

/39/ Caillibot P.F., Wyatt B.S., AECL-3472 (1969)

/40/ Feraday M.A. et al., Nucl. App. 4 (1968) 148

/41/ Feraday M.A. et al., AECL-3111 (1969)

/42/ Feraday M.A. et al., AECL-4058 (1974)

/43/ Feraday M.A. et al., AECL-5028 (1975)

/44/ Hasting I.J., Stoute R.F., J. Nucl. Mat. 37 (1970) 295

/45/ Hasting I.J., J. Nucl. Mat. 41 (1971) 195

/46/ Bethune B., J. Nucl. Mat. 40 (1971) 205

/47/ Pellissier J. et al., J. Nucl. Mat. 43 (1972) 93

/48/ Bleiberg M.L., Jones L.J., Trans. AIME 209 (1957) 1236

/49/ Bethune B., J. Nucl. Mat. 31 (1969) 197

/50/ Katz N.H., Binstock M.H., NAA-SR-6226 (1962)

/51/ Accary A., Caillat R., J. Am. Cer. Soc. 45 (1962) 347

/52/ Steinkopff H., Bericht über die II. Int. Pulvermet. Tagung
      Eisenach 1961, Abhandlung der Deutschen Akademie der Wissen-
      schaften zu Berlin, (1962) 185 ff

/53/ Taylor K.M., McMurty C.H., ORO-400 (1961)

/54/ Thurber W.C., Beaver R.J., ORNL-2602

/55/ Thurber W.C. et al., ORNL-2351 (1958), (1959)

/56/ Boucher R., J. Nucl. Mat. 1 (1959) 14

/57/ Exner H.E., Petzow G., Proc. 5th Internat. Leichtmetalltagung
      Leoben (1968) 78

/58/ Petzow G., Kvernes I., Z. für Metallkunde 52 (1961) 698

/59/ Petzow G., Kvernes I., Z. für Metallkunde 53 (1962) 248

/60/ Zelenzny W.F., Nucl. Appl. 2 (1966) 239

/61/ Holden A.N., "Dispersion fuel elements", (1968) (Gordon and Breach)

/62/ White D.W. et al., TID-7546, Book 2, (1957)

/63/ Martin M.M. et al., ORNL-4856 (1973)

/64/   Jesse A. et al.,   Powder Metallurgy 14 (1971) 289

/65/   Dienst W., KfK-Ext. 6/67-1 (1967)

/66/   Nazaré S. et al.,   J. Nucl. Mat. 56 (1975) 251

/67/   Dienst W. et al., J. Nucl. Mat. 64 (1977) 1

/68/   Gibson G.W.,   IN - 1133 (1967)

/69/   Francis W.C.,   IDO-17 154 (1966)

/70/   Walker V.A. et al.,   IDO-17 157 (1966)

/71/   Williams J.,   AERE-M-1974 (1956)

/72/   Rollig H.E.,   Kernenergie 5 (1962) 809 and Kernenergie 6 (1963) 685

/73/   Waugh R.C.,   ORNL-2701 (1959)

/74/   Ondracek G.,   Metall (May issue)(1982)

/75/   Ondracek G., Nikolopoulos P., Pulvermetallurgie-Konferenz,
        Florenz (1982)

/76/   Ondracek G., Schulz B.,   J. Nucl. Mat. 46 (1973) 253

Property	U_3Si	Ref.	U_3Si_2	Ref.
Melting point (K)	1198 (decomposes)	/13/	1938	/13/
Crystal structure	tetragonal f.c. (≤1038 K) a = 602.9 pm c = 869.6 pm cubic a = 434.6 pm 1038 - 1198 K	/15/ /14/	tetragonal a = 732.99 pm c = 390.04 pm	/15/
Density (g cm^{-3})	15.58		12.2	
U-density (gU cm^{-3})	14.98		11.31	
Molar heat (c_p) (J mol^{-1} K^{-1}	T (K) 300 500 1000 110.3 132.6 142.0	/16/	T (K) 300 500 1000 131.0 156.6 168.4	/16/
Enthalpy (KJ mol^{-1})	-91.9 -67.0 2.4	/16/	-170.6 -141.2 -59.0	/16/
Gibbs energy (KJ mol^{-1})	-142.3 -182.6 -324.6	/16/	-320.1 277.7 445.5	/16/
Thermal conductivity (W cm^{-1} K^{-1})	0.175 T = 332 K	/17/	0.084 T = 338 K	/18/
Mean linear coefficient of thermal expansion (K^{-1})	$13.0 \cdot 10^{-6}$ (293-473 K) $16.8 \cdot 10^{-6}$ (293-973 K)	/19/	$15.5 \cdot 10^{-6}$ (293-473 K) $15.1 \cdot 10^{-6}$ (293-973 K)	/19/
Young's modulus (KN/mm^2)	154		51-142	
Microhardness (VPN) VPN at 0.5 N	U_3Si 180 - 200 200 ± 6	/39/ this work	U_3Si_2 600 - 700 550 ± 30	/39/ this work

Table I: Some properties of U_3Si and U_3Si_2.

Vol.% U_3Si or U_3Si_2	Composition (Nominal) at.%			Phases identified		Lattice Parameter pm (Heat treated)	Analysis (Microprobe) at.%			Micro-hardness VPN (Load 0.05 N)
	U	Si	Al	as cast	Heat treated (873 K, 33 d)		U	Al	Si	
20	13.00	4.33	82.67	U(Si,Al)$_3$ Al(Si)	U(Si,Al)$_3$ UAl$_4$(Si) Al(Si)	426.3±0.2 a = 440.7, b = 627.4 c = 1371.0 405.8±0.1				310±50 197±35
30	19.83	6.61	73.56	U(Si,Al)$_3$ Al(Si)	U(Si,Al)$_3$ UAl$_4$(Si)	426.3±0.1 a = 440.2, b = 626.1 c = 1372.1	27 20	71 71	2 9	298±37 195±15
40	26.90	8.95	64.15	U(Si,Al)$_3$ UAl$_2$(Si)	U(Si,Al)$_3$ UAl$_2$(Si)	425.3±0.2 773.4±0.3				280±42 344±28
50	34.23	11.38	54.39	U(Si,Al)$_3$ UAl$_2$(Si) U$_3$Si$_2$(Al)	U(Si,Al)$_3$ UAl$_2$(Si) U$_3$Si$_2$(Al)	425.3±0.1 771.5±0.3	27 34 44	59 60 17	14 6 39	439±100 399±33
20	9.92	6.59	83.49	U(Si,Al)$_3$ Al(Si)	U(Si,Al)$_3$ Al(Si)	423.9±0.2 405.8±0.1				290±15 12±2
30	15.19	10.12	74.69	U(Si,Al)$_3$ Al(Si)	U(Si,Al)$_3$ Al(Si)	424.1±0.2 405.8±0.1				247±32 23±5
40	20.72	13.80	65.48	U(Si,Al)$_3$ Al(Si)	U(Si,Al)$_3$ Al(Si)	424.1±0.2 405.3±0.4				350±40 42±5
50	26.50	17.60	55.90	U(Si,Al)$_3$ USi$_3$(Al) U$_3$Si$_2$(Al)	U(Si,Al)$_3$ USi$_3$(Al) U$_3$Si$_2$(Al)	425.2±0.3	26 44	57 17	17 39	306±47

(Left margin labels: U_3Si-Al for the upper four rows, U_3Si_2-Al for the lower four rows)

Table III: X-ray diffraction, microhardness and mircorprobe analysis of U_3Si/U_3Si_2-Al samples.
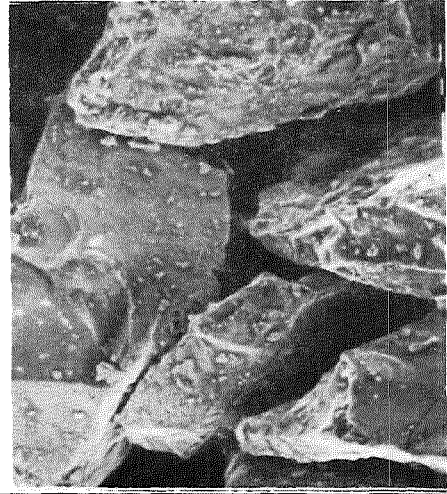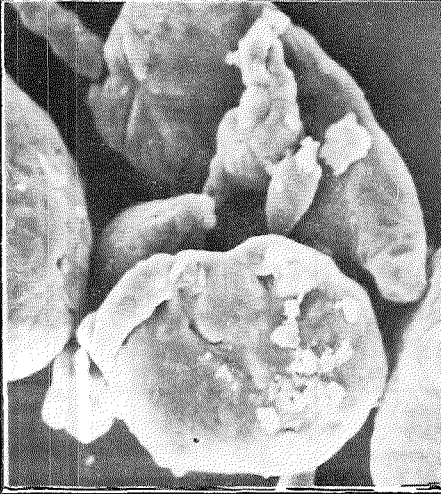
Chemical composition (wt.-%)	U_3Si	U_3Si_2	Al
Al	-	-	99.5
C	0.11	0.12	-
Fe	-	-	0.13
H_2	-	-	0.011
N_2	<0.01	<0.01	-
O_2	~0.3	0.23	0.29
Si	4.0 (nom)	7.4 (nom)	0.07
Particle size (μm)	63-90	63-90	18.6 (mean)
Particle shape			

Table II: Chemical composition and powder characteristics of U_3Si, U_3Si_2 and Al.
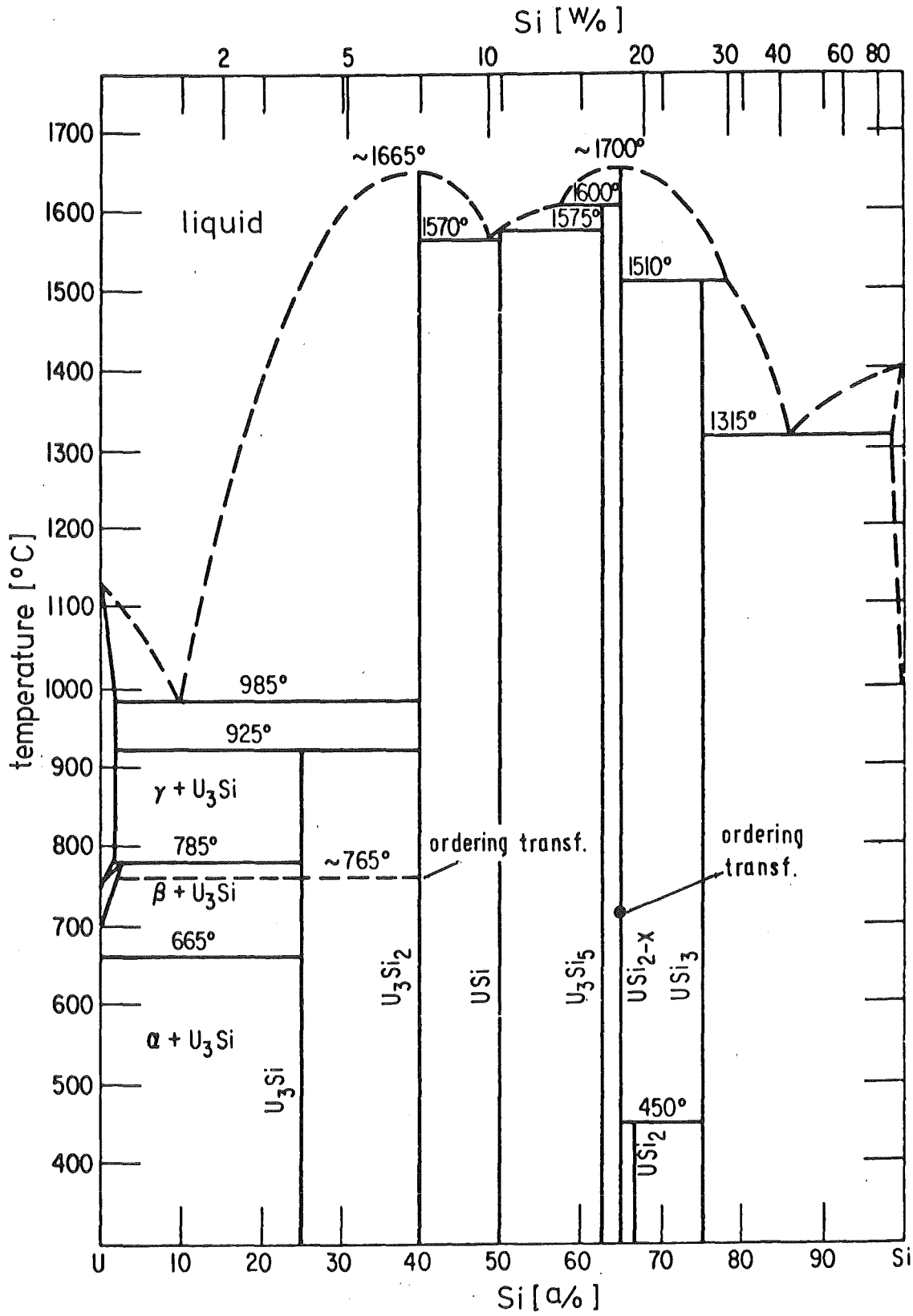
Fig.1: The U-Si phase diagram /from 10/.
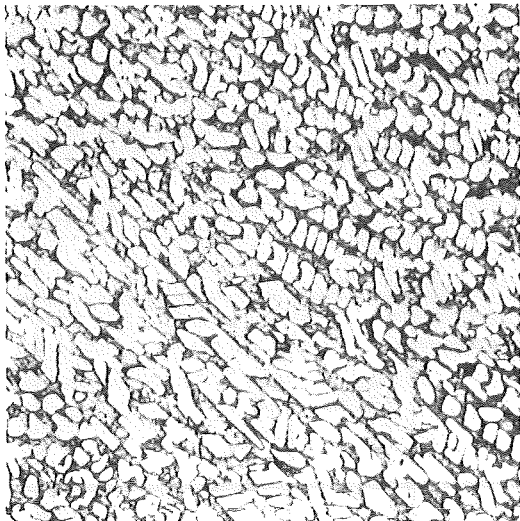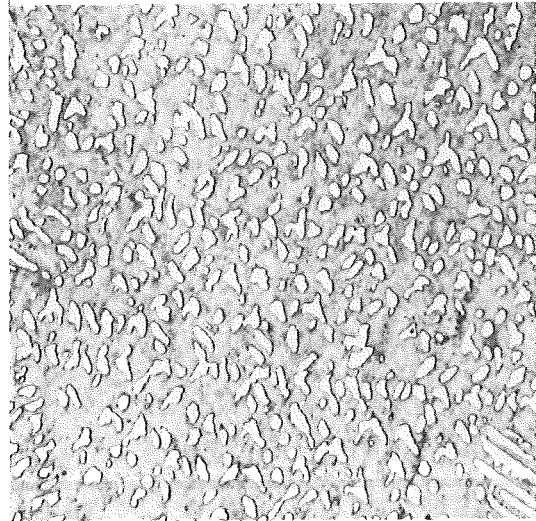
a)   after melting   b)   homogenised

ARC MELTING
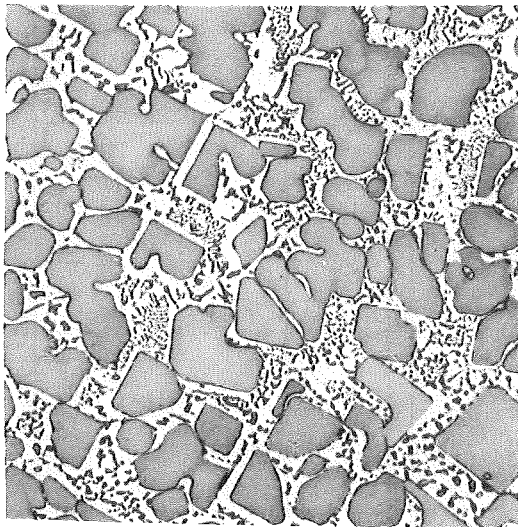
c)   after melting   d)   homogenised

INDUCTION MELTING

├────┤ 50 µm
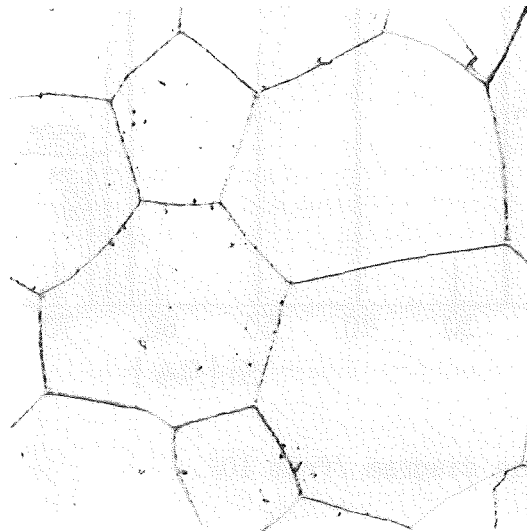
├────┤ 10 µm

e) homogenised (grain boundary etch)

Fig.2:   Microstructures of U_3Si (nominally 4 wt.-% Si) as molten and
          homogenised (1073 K, 72 hours, $<10^{-5}$ mbar) prepared by induc-

- 29 -

a)   as molten
ARC MELTING

50 μm

b)   as molten
INDUCTION MELTING

100 μm

c)   homogenised (grain boundary etch)

Fig.3: Microstructures of U_3Si_2 (nominally 7.4 wt.-% Si) - as molten -
and homogenised (1073 K, 72 hours, $<10^{-5}$ mbar) prepared by in-
duction and arc melting.
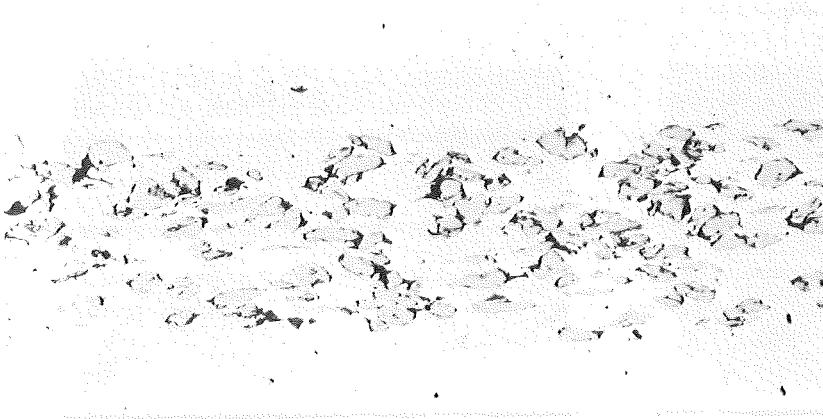
3.0 g U/cm^3
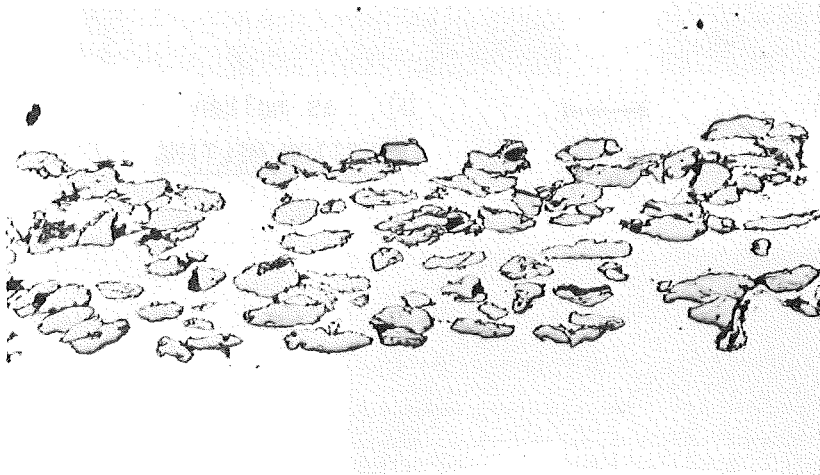
4.0 g U/cm^3
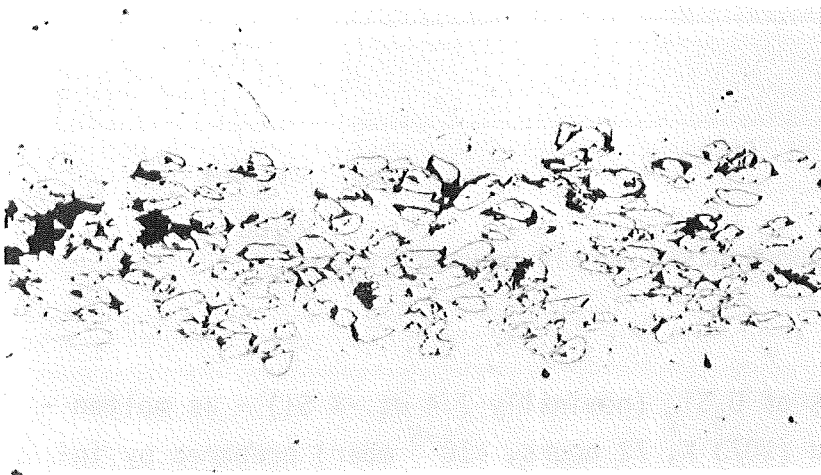
6.0 g U/cm^3

200 µm

Fig.4a: Microstructure of U$_3$Si-Al fuel plates.
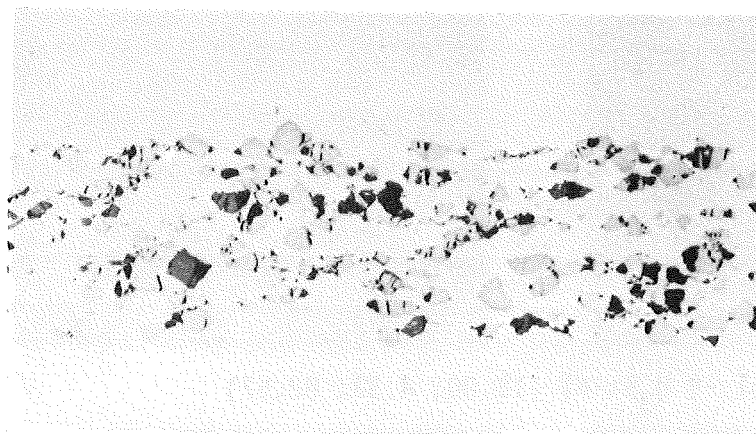
3.0 g U/cm^3
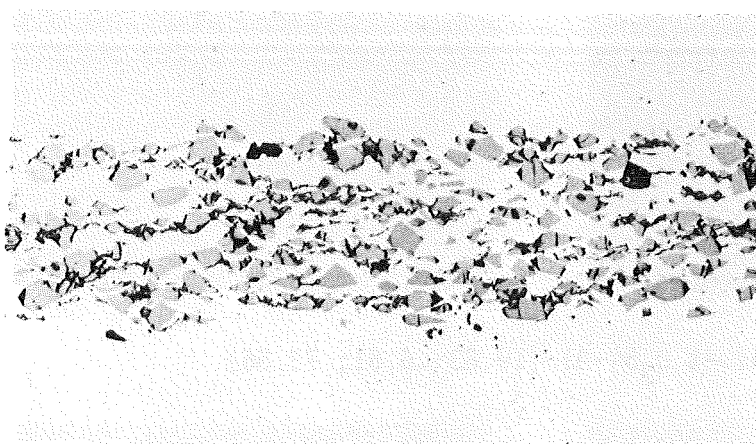
4.0 g U/cm^3

4.5 g U/cm^3
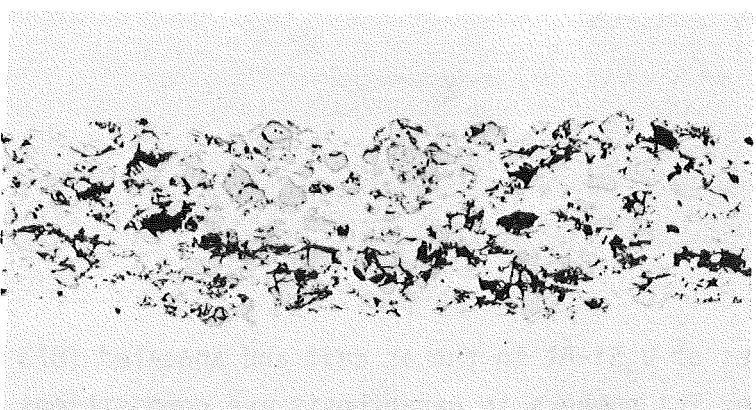
4.75 g U/cm^3
from NUKEM

⊢————⊣

200 μm

Fig.4b: Microstructure of U$_3$Si$_2$-Al fuel plates.

a)

b)

c)   20 vol.-% U$_3$Si-Al (13.00; 4.33; 82.67)   d)

e)   30 vol.-% U$_3$Si-Al (19.83; 6.61; 73.56)   f)

g)   40 vol.-% U$_3$Si-Al (26.90; 8.95; 64.15)   h)

50 vol.-% U$_3$Si-Al (34.23; 11.38; 54.39)   ⊢————⊣
                                                                20 µm
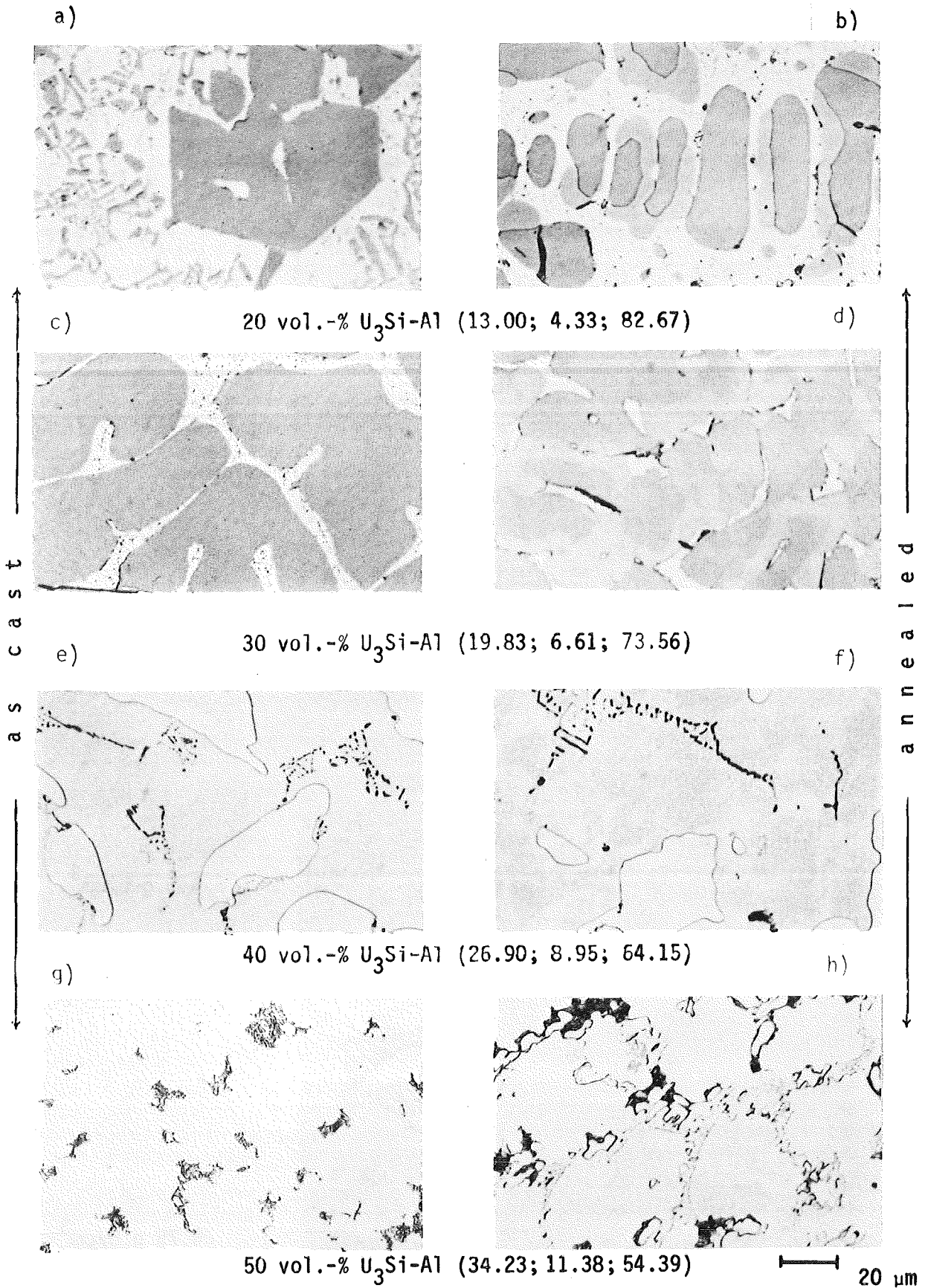
Fig.5: Microstructures of U$_3$Si-Al in the as cast and annealed (873 K, 33 days) state. The numbers in parenthesis are compositions in at.-% of uranium, silicon and aluminium.

a) 90 mol.-% UAl_3 - 10 mol.-% USi_3

20 μm
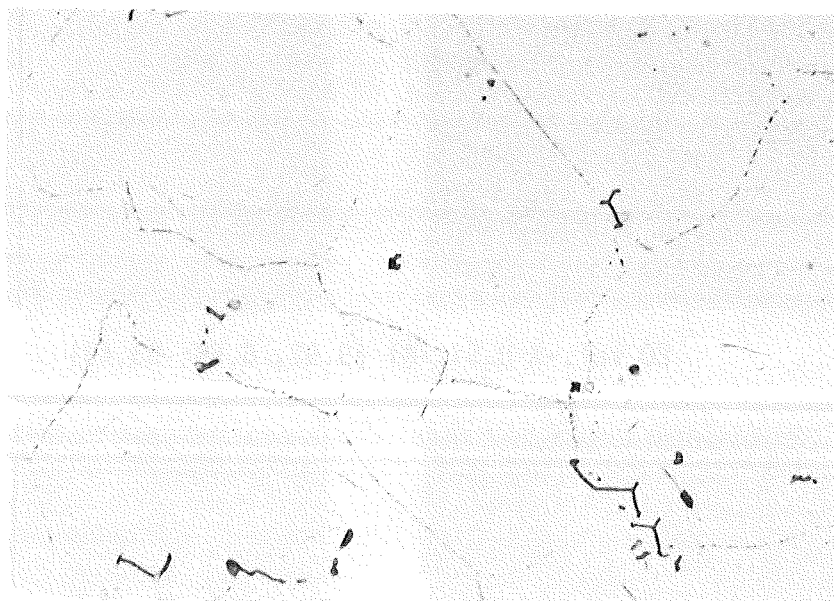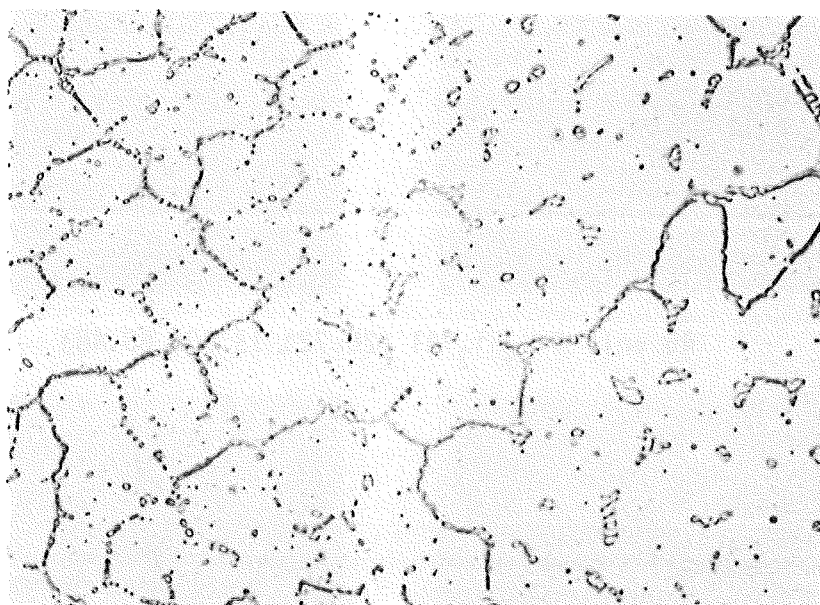
b) 70 mol.-% UAl_3 - 30 mol.-% USi_3

Fig.6: Microstructures of annealed samples (1123 K, 15 days) showing precipitation of a silicon rich UAl_3 phase.

a)

b)

20 vol.-% U$_3$Si$_2$-Al (9.92; 6.59; 83.49)

c)

d)

30 vol.-% U$_3$Si$_2$-Al (15.19; 10.12; 74.69)

e)

f)

40 vol.-% U$_3$Si$_2$-Al (20.72; 13.80; 65.48)

g)

h)

50 vol.-% U$_3$Si$_2$-Al (26.50; 17.60; 55.90)   ⊢——⊣ 20 µm
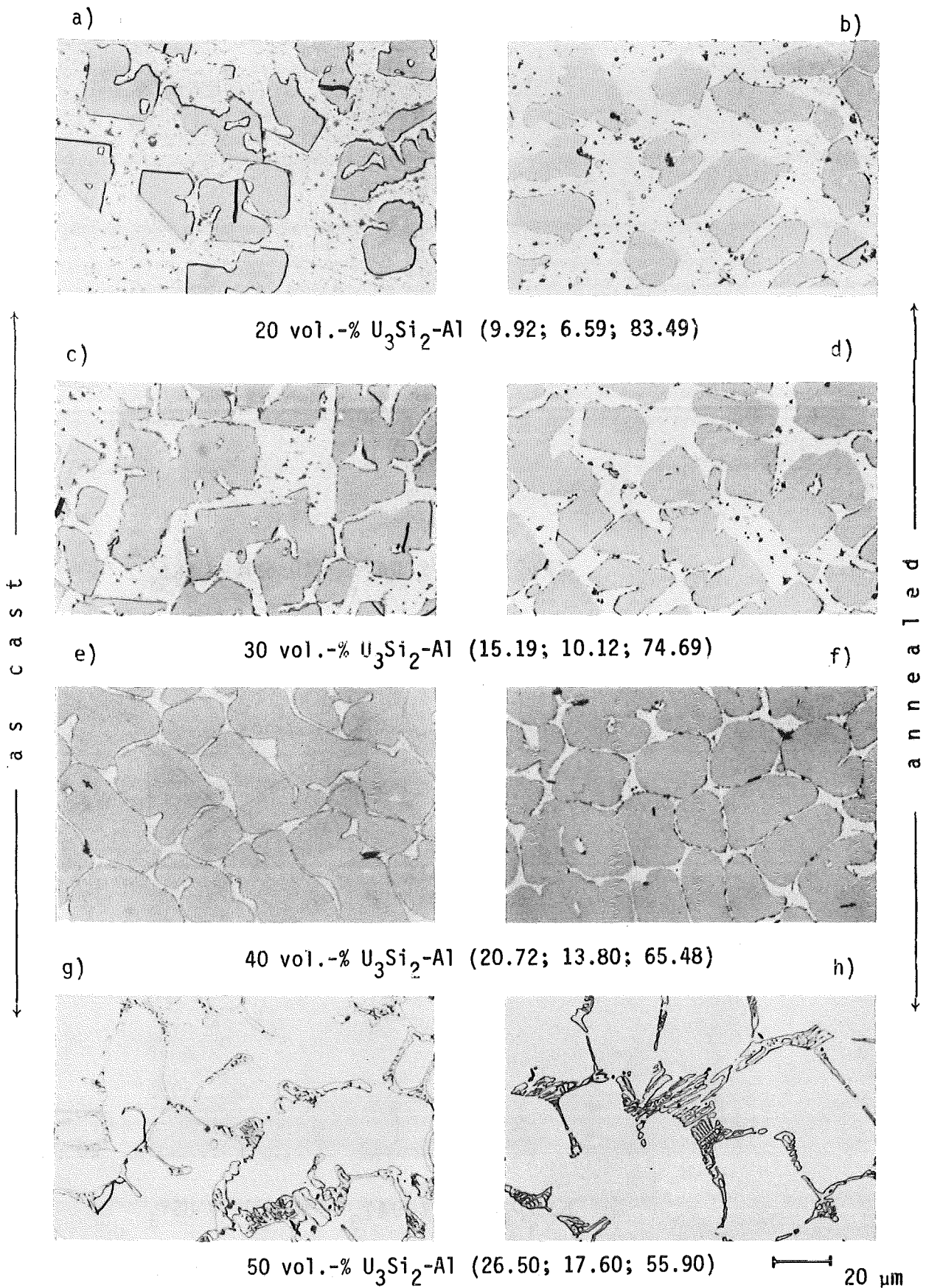
as cast

annealed

Fig.7:   Microstructures of U$_3$Si$_2$-Al in the as cast and annealed (873 K, 33 days) state. The numbers in parenthesis are compositions in at.-% of uranium, silicon and aluminium.
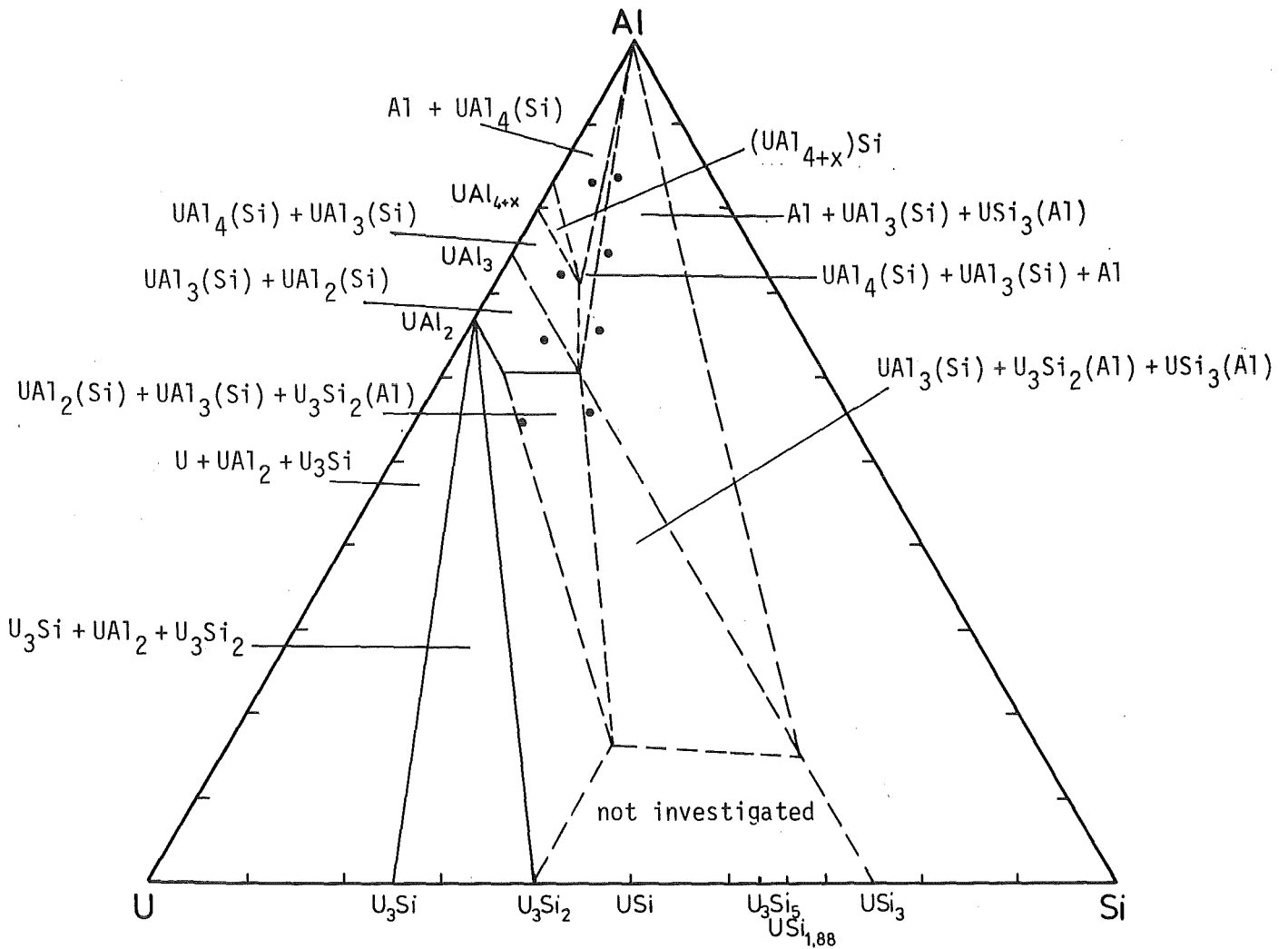
Fig.8: Tentative isothermal section at 873 K in the U-Si-Al system.
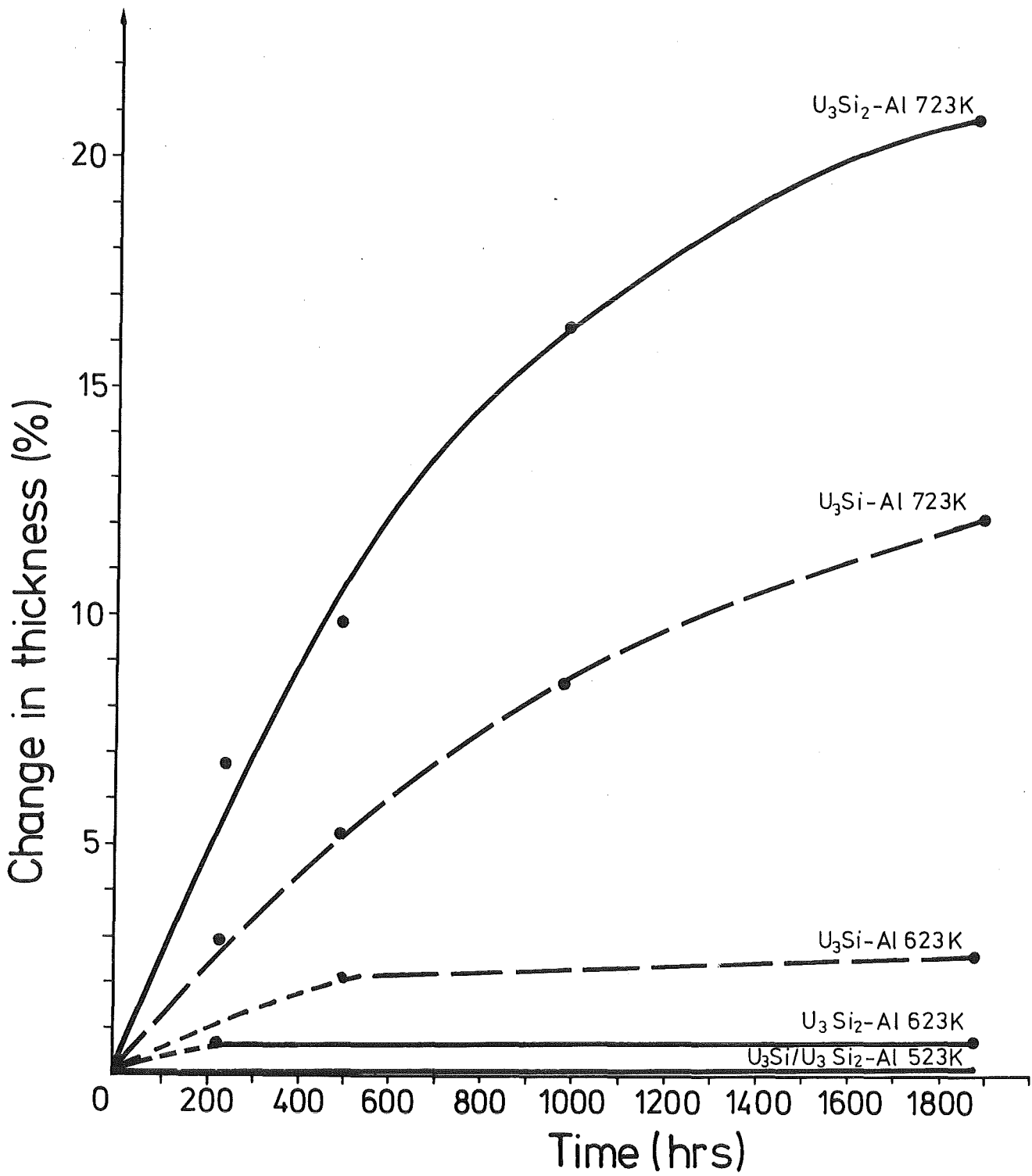
Fig.9:   Change in thickness of roll bonded U_3Si- and U_3Si_2-Al fuel plates
          (4.0 g U/cm^3) after heat treatment.

U$_3$Si-Al   U$_3$Si$_2$-Al
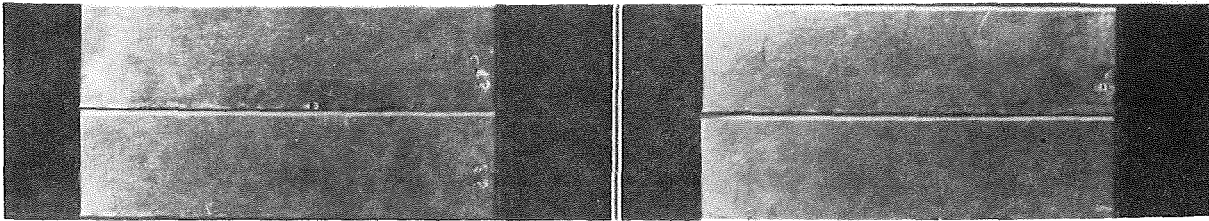
a)   b)

2000 h, 250°C
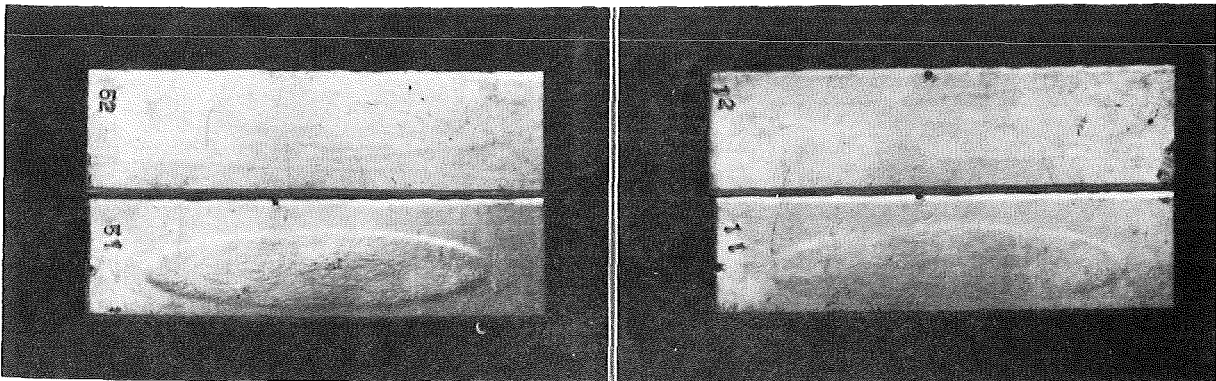
c)   d)

2000 h, 350°C
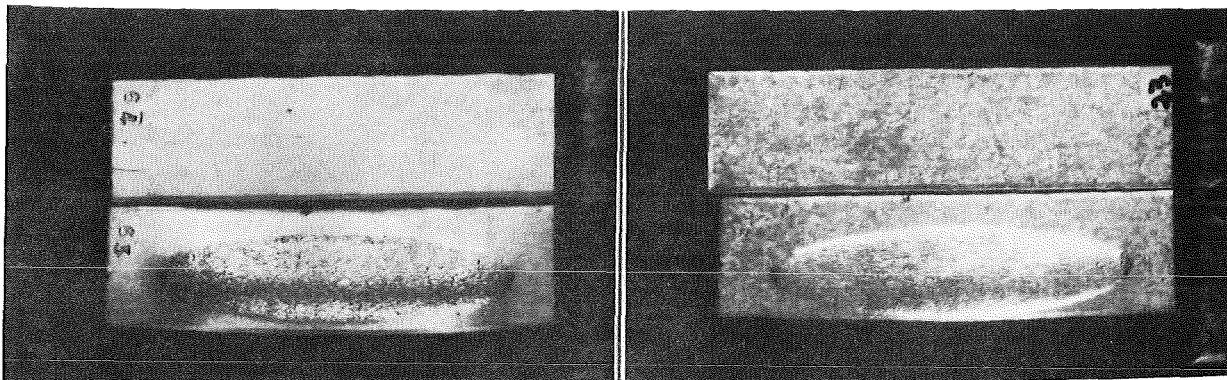
e)   f)

2000 h, 450°C

Fig.10:   Selected U$_3$Si- and U$_3$Si$_2$-Al fuel plates (4.0 g U/cm^3) after heat treatment.
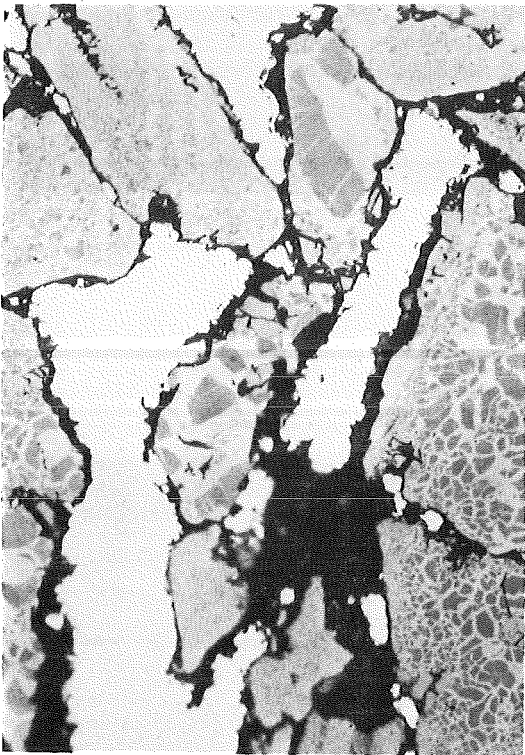
723 K/200 h
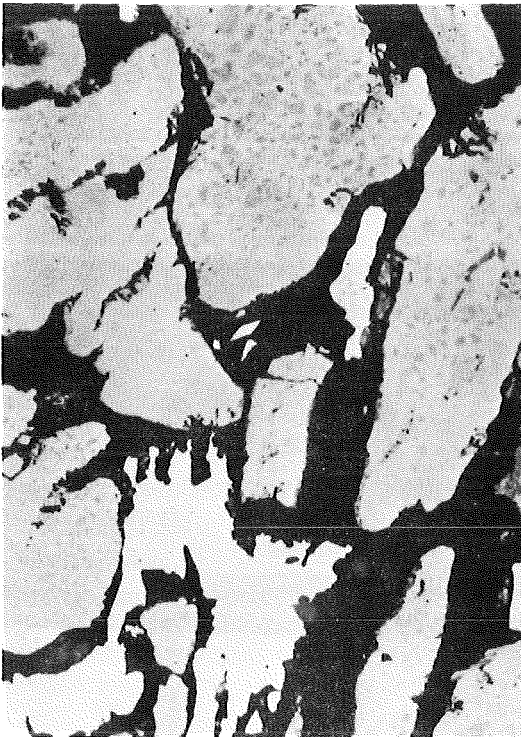
723 K/500 h
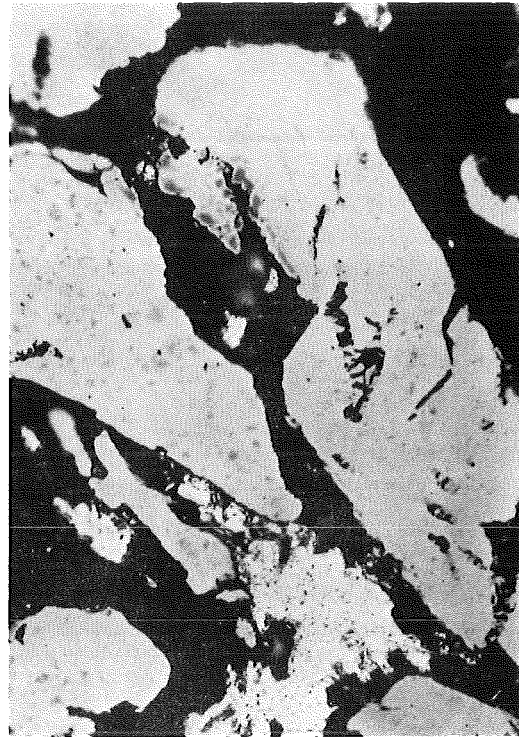
723 K/1000 h

723 K/2000 h

20 µm

Fig.11: Microstructures of U_3Si-Al fuel plates (4.0 g U/cm^3) after heat treatment.
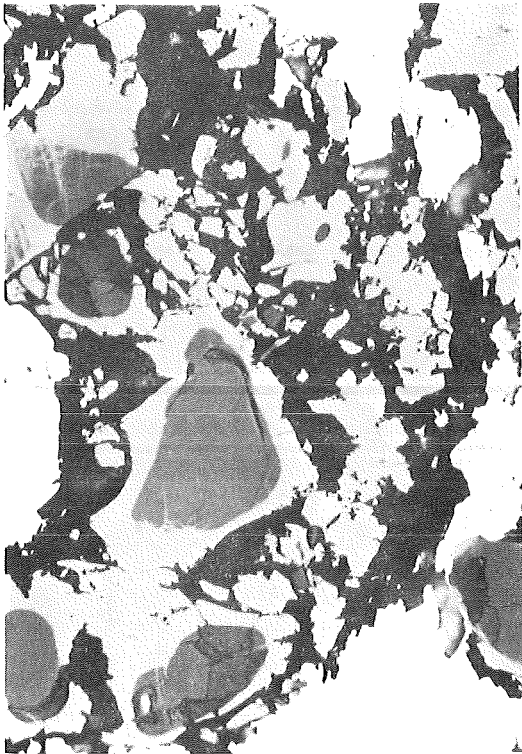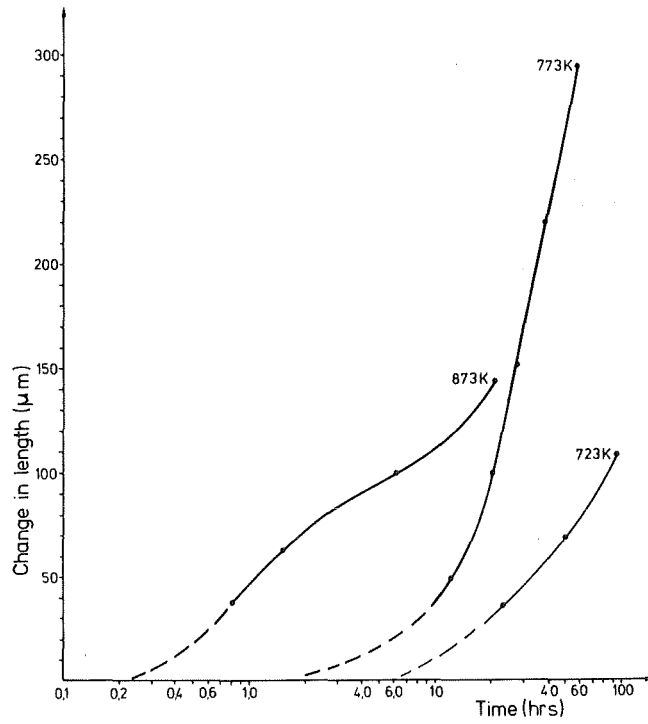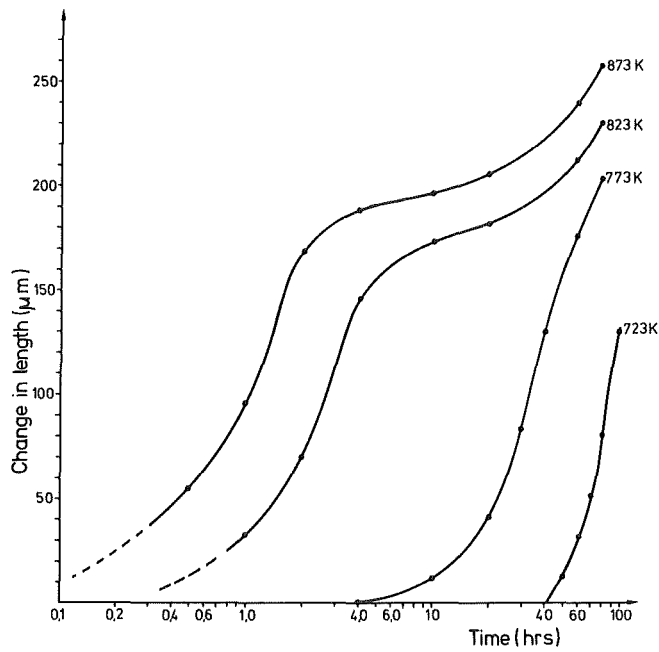
723 K/200 h

723 K/500 h

723 K/1000 h
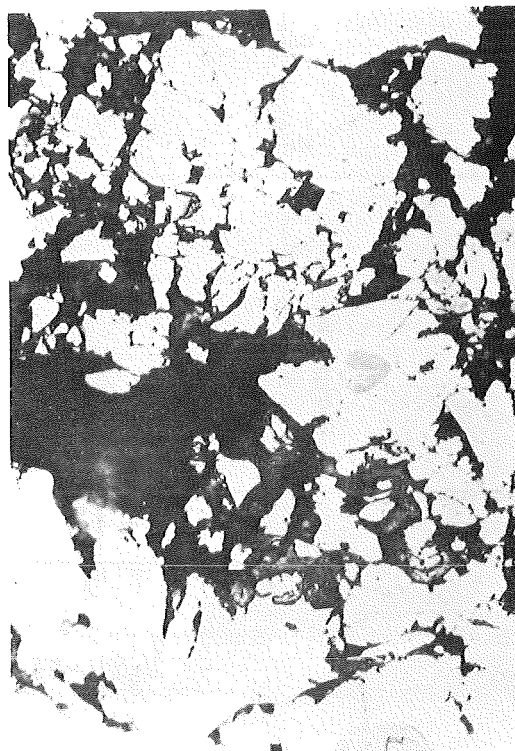
723 K/2000 h

20 µm

<u>Fig.12:</u>   Microstructures of U_3Si_2-Al fuel plates (4.0 g U/cm^3)
after heat treatment.

U_3Si-Al (4.0 g U/cm^3)

U_3Si_2-Al (4.0 g U/cm^3)

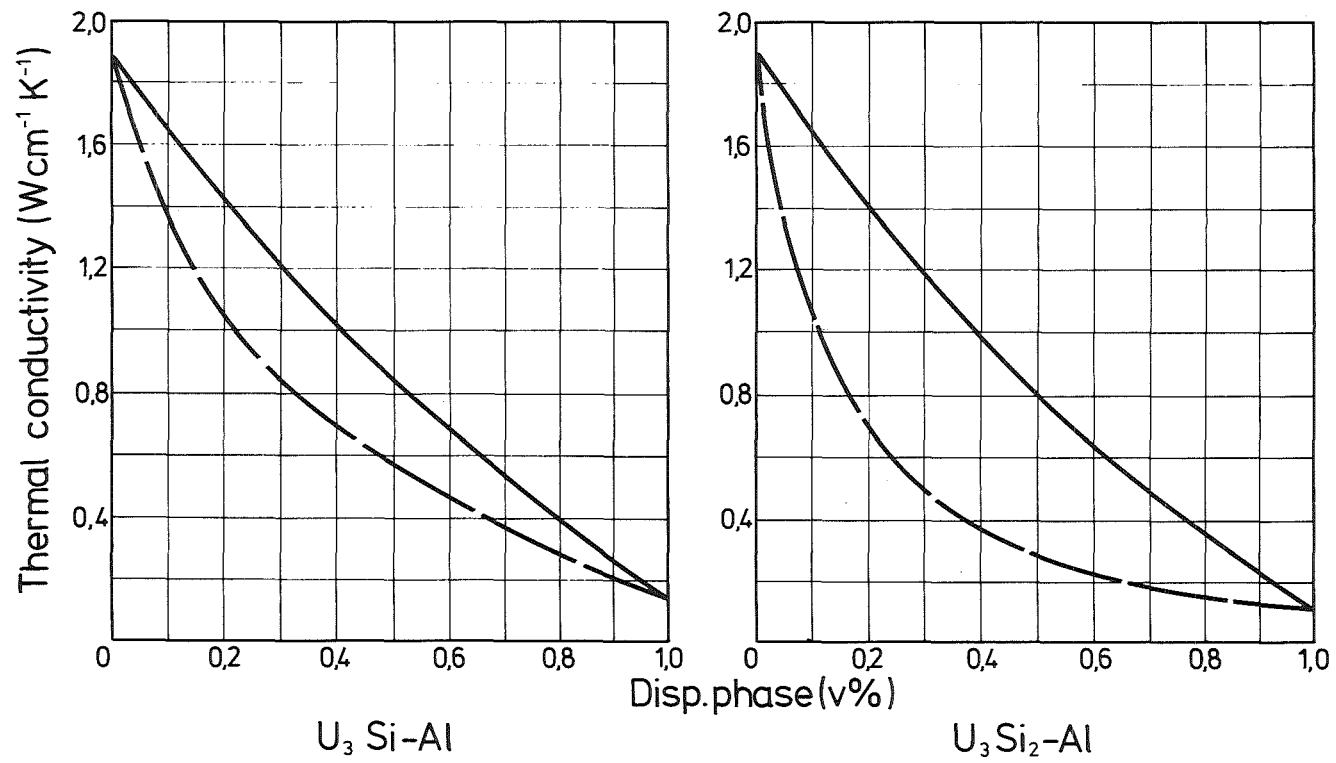Fig.13:   Isotherms of dilatometric variation of thickness of U_3Si- and U_3Si_2-Al fuel plates.

Fig.14:   Bounds of the thermal conductivity of theoretically dense U_3Si- and U_3Si_2-Al dispersions.